Electrochemical regeneration of a graphite adsorbent loaded with Acid Violet 17 in a spouted bed reactor

Dun Liu, E.P.L. Roberts, A.D. Martin, S.M. Holmes, N.W. Brown, A.K. Campen, N. de las Heras

PII: S1385-8947(16)30877-4
DOI: http://dx.doi.org/10.1016/j.cej.2016.06.070
Reference: CEJ 15380

To appear in: *Chemical Engineering Journal*

Received Date: 24 March 2016
Revised Date: 10 June 2016
Accepted Date: 11 June 2016

Please cite this article as: D. Liu, E.P.L. Roberts, A.D. Martin, S.M. Holmes, N.W. Brown, A.K. Campen, N. de las Heras, Electrochemical regeneration of a graphite adsorbent loaded with Acid Violet 17 in a spouted bed reactor, *Chemical Engineering Journal* (2016), doi: http://dx.doi.org/10.1016/j.cej.2016.06.070

Electrochemical regeneration of a graphite adsorbent loaded with Acid Violet 17 in a spouted bed reactor

Dun Liu[a,*], E.P.L Roberts[b], A.D. Martin[c], S.M. Holmes[a], N.W. Brown[d], A.K. Campen[d], N. de las Heras[d]

a School of Chemcial Engineering and Analytical Science, The University of Manchester, M13 9PL,UK

b Department of Chemcial and Petroleum Engineering, Univeristy of Calgary, T2N 1N4, AB,Canada

c Department of Chemical Engineering, Lancaster University, LA1 4YR,UK

d Arvia Technology Limited, The Heath Business and Technical Park, Cheshire, WA7 4EB

**Corresponding author Tel:+447719774392*

E-mail:dun.liu@postgrad.manchester.ac.uk

Highlights

- A two-phase reactor is a promising alternative to traditional three-phase reactor.
- The spouted bed region defined an interesting operating domain.
- Study of current density and the liquid flow rate on the system performance.
- A model is developed for the adsorption and electrochemical regeneration process.

Abstract

A novel spouted bed reactor is evaluated for water treatment by an adsorption and electrochemical regeneration process. The adsorbent is a bisulphate graphite intercalation compound with low specific surface area but high electrical conductivity, suitable for adsorption of contaminants and simultaneous electrochemical regeneration within a single unit. The effects of current density and liquid flow rate on Acid Violet 17 removal were investigated. The hydrodynamic behavior of the liquid spouted bed reactor was characterized by a flow regime map. A four-parameter model has been developed to describe the adsorption and electrochemical regeneration process in the liquid spouted bed reactor. It was found that the experimental data of dye removal agrees well with the modelled simulations.

Keywords

Adsorption; Electrochemical regeneration; Acid Violet 17; Graphite intercalation compound; GIC; Spouted bed reactor

1. Introduction

Adsorption technology is widely used for the removal of organic and inorganic contaminants from water and wastewater. Many absorbents are in use, among which activated carbon is the most widely used for removal organic pollutants. Once the activated carbon has been exhausted, it must either be regenerated, typically by an energy intensive thermal process, or disposed of, which is economically and environmentally unattractive [1].

There are two approaches suggested by many researchers to resolve the problems related to the exhausted activated carbon. The first is to develop low cost natural adsorbents that can be used once, such as using orange peel [2], plum kernels [3] and sunflower seed hull [4], etc. However, this approach only transfers the pollutant from the liquid to solid phase [5]. The

second is by regenerating the adsorbent. Among regeneration methods, thermal regeneration is the choice for most industrial applications. This method, however, has high energy consumption (operating temperatures are 800 ~ 850 ℃), and leads to 5~15% carbon loss due to oxidation and attrition [6]. Therefore, alternative regeneration methods have been investigated by researchers, including microwave [7], ultrasound [8], biological [9], Fenton oxidation [10], wet air oxidation [11] and electrochemical [12-15].

Electrochemical regeneration has been found to be effective for the regeneration of activated carbon, which can achieve regeneration efficiencies of 80-99% [12-15]. However, the adsorption and regeneration process was slow because of the limited rate of intra-particle diffusion. Thus long adsorption and regeneration times are required [5]. For example Zhang [12] reported that 24h was required to achieve adsorption equilibrium and 5h was needed for 85.2% electrochemical regeneration for granular activated carbon.

An alternative approach was investigated by using a non-porous, highly-conducting graphite-based adsorbent material, a flake graphite intercalation compound (GIC) [5]. Because this adsorbent lacks internal surface area, it can significantly reduce the adsorption and regeneration time, but has a low adsorbent capacity. Anodic regeneration leads to oxidation of organic adsorbates on the surface of the GIC. The rapid adsorption and electrochemical regeneration have allowed the design of a treatment process that can adsorb contaminants and electrochemically regenerate adsorbents simultaneously within a single unit [16].

Most previous work exploited air-lift fluidized bed reactors for waste water treatment by adsorption and electrochemical regeneration [16,17]. This is because fluidized beds have certain unique characteristics such as enhanced mass transfer rates, high mixing rates and homogeneous reaction conditions [18]. However, their disadvantages are the possibility of

forming a bubbling regime which would lead to non-uniform current distribution and high ohmic drop, i.e. increasing the energy consumption [17]. Mathur and Gishler [19] developed a spouted bed which can effectively deal with coarse particles with the same efficiency as a conventional fluidized bed. Since then, spouted beds have been used extensively in wheat drying, coating, granulation, coal gasification, combustion and wastewater treatment [20].

A novel spouted bed electrochemical reactor (SBER) for water treatment by an adsorption and electrochemical regeneration process is described in this work. Water to be treated is introduced at discrete locations to obtain a regular cyclic motion of particles in the spouted bed, to improve the mixing efficiency between fluid and particles [19,21-23]. The spouted bed has the advantage that parts of the bed are remain as a close packed moving bed, allowing the passage of current through the bed of adsorbent without the problems associated with intermittent contact that arise in a fluidised bed [17]. The main objective of the present study, therefore, is to evaluate the treatment of a model effluent by adsorption and electrochemical regeneration in an SBER under a range of operating conditions, to study the hydrodynamics of the spouted bed, and to develop a reactor model of the SBER.

2. Materials and methods

2.1. Materials

2.1.1 Adsorbent

The adsorbent used in this study was a bisulphate GIC and was supplied by Arvia Technology Ltd under the trade name Nyex™ 1000. This material has been used in several previous studies of adsorption/electrochemical regeneration process [16,24]. The particles of adsorbent have a characteristic flake like appearance (Fig.1) associated with the graphite precursor. GIC is more hydrophilic than graphite flake, and has surface functional groups [25] that enhance the adsorption performance. The GIC used in this study had a carbon

content of about 95% w/w, a density of 2.225 g cm^{-1} with particle diameters of 100 to 700 µm, and mean particle diameters of around 500 µm [16]. All particles of size less than 140 µm were sieved out to avoid leaving the reactor because of the small particle size. Based on nitrogen adsorption, the value of Brunauer Emmet Teller (BET) surface area was determined to be 1.0 m^2g^{-1}. This is very low compared with typical activated carbons with surface area in the range 600-2000 m^2g^{-1} [26]. By mercury porosimetry, it was revealed that essentially no internal pores existed in the material. GIC has a high concentration of free electron carriers at room temperature leading to a relatively high bed electrical conductivity of 0.16 $(\Omega \cdot cm)^{-1}$ compared to around 0.025 $(\Omega \cdot cm)^{-1}$ for GAC [5].

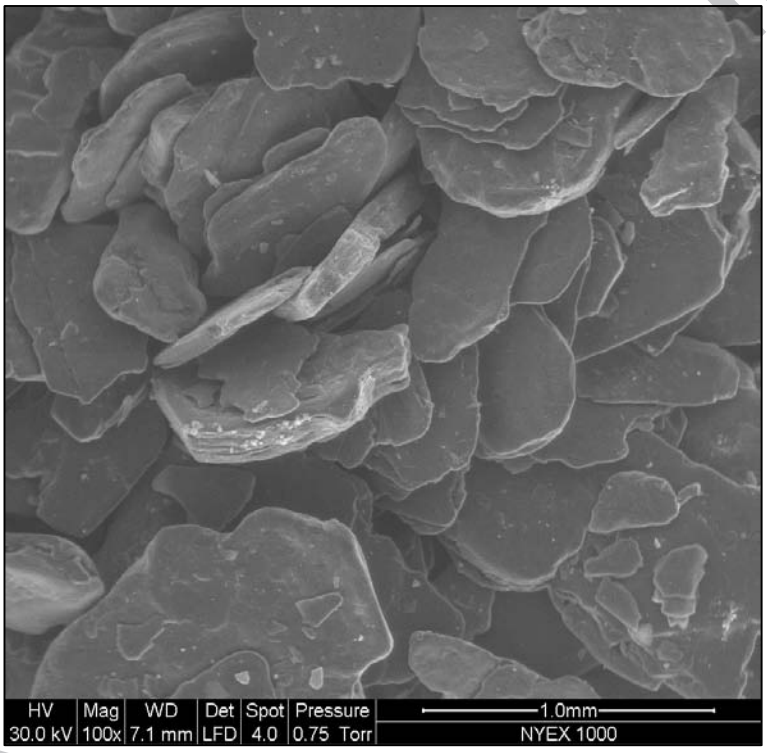

Fig. 1. SEM micrograph of the GIC adsorbent used in this study (Nyex™1000)

2.1.2 Adsorbate

Acid Violet 17 (AV 17) was used as the adsorbate in this study and was supplied by Sigma-Aldrich Company Ltd UK under the trade name Coomassie® Violet R200. It was

chosen as the target compound because it has low toxicity and used in previous studies [16]. It is commercial grade and was used in the experiments without further purification. The supplier indicated that the AV 17 content of the Coomassie® Violet R200 was 50%, the remainder is an inorganic salt used in the dye manufacture process. The dye content was confirmed by total organic carbon (TOC) analysis. The AV 17 solutions were prepared using distilled water and mixing for 30 min. The chemical structure and the characteristics of AV 17 are shown in Table 1.

Table 1

The physical and chemical characteristic of the Acid Violet 17 used in this study

Generic Name	Acid Violet 17
Color index	42650
Molecular Formula	$C_{41}H_{44}N_3NaO_6S_2$
Molecular Weight	761.93
Purity	50% (the remainder is inorganic salt)
Chromophore	Triphenyl methane
λ_{max}(nm)	542
Molecular Structure	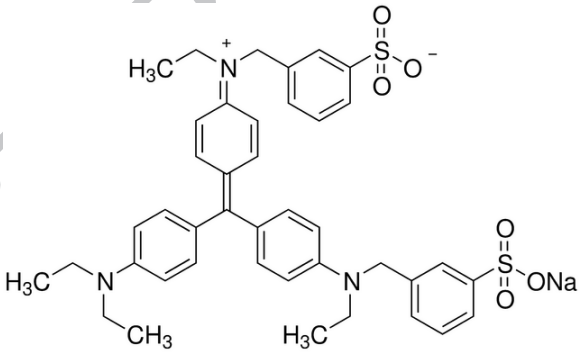

λ_{max}: wavelength of maximum absorbance

2.2. Experimental set up and procedures

The removal of colour from wastewater and the electrochemical regeneration of the GIC adsorbent were performed in a liquid-lift cell at ambient laboratory temperature of 20°C and atmospheric pressure. A schematic diagram of the experimental set up is shown in Fig.2. This

reactor operated with simultaneous adsorption and electrochemical regeneration occurring within a single unit. The main body of the Liquid-Lift reactor consisted of two rectangular sheets of transparent polyvinyl chloride (PVC) of 6 mm thickness (see Fig.3 (a)) and the internal dimensions of the process unit were 40 cm tall, 20 cm wide and 2.5 cm deep. Two liquid inlets were provided on either side of the lower sidewalls of the unit. The adsorbent (solid phase) formed a bed at the bottom of the anodic chamber. The liquid to be treated was injected into an inlet chamber below the anodic chamber and distributed through a perforated plate (see Fig.3 (c)), which had four equidistant inlets, each of diameter 1 mm. During operation liquid and solid phases flowed concurrently to the top of the adsorbent bed where they were separated under gravity, with the solid phase circulating back to the base of the reactor and the liquid phase flowing over a weir at the top of the reactor to provide a uniform flow at the outlet. For the range of flowrates used, the 35 cm high chamber above the anode compartment was found to be sufficient to separate the adsorbent particles so that no particles flowed over the weir.

The lower outside of the anode chamber was fitted with a graphite plate (20 cm wide by 5 cm tall) which formed the anode current feeder. The adsorbent in contact with the graphite plate was thus anodic, and was separated from a stainless steel cathode (316L perforated with 3mm holes, 33% open area, 1mm thickness) by means of a micro porous polyethylene membrane (Daramic 350, Grace GmbH Germany). The anodic conditions in the adsorbent bed leads to electrochemical oxidation of the adsorbed AV17, regenerating the adsorbent. The cathode was directly adjacent to the membrane and the distance between the graphite plate and the membrane was 2 cm (Fig. 3 (b)). The projected area of the anode current feeder, separator and cathode were 20×5 cm. The catholyte in the cathode compartment was acidified 0.3% w/w NaCl solution. The catholyte was acidified using 37% HCl solution to pH

2 to neutralise any hydroxide formed due to water electrolysis and to maintain the conductivity of the separator, which is highest at low pH.

The batch, simultaneous method comprises a single multi-step phase in which a quantity of AV 17 is contacted with a fixed mass of GIC whilst the adsorbent is simultaneously being electrochemically regenerated under constant current conditions. A volume of 4 L of water containing 100 mg L^{-1} AV 17 solution was charged to the reservoir. The anode compartment of the liquid-lift cell was then partially filled from the reservoir and a mass of 140 g of GIC was added. A recirculating flow of AV 17 solution was established simultaneously with the selected regeneration current and the start of the timer. The DC current was maintained at a constant value throughout each experiment. Samples were taken from the outlet of the liquid-lift reactor every 10 min until the colour was completely removed. These samples were centrifuged and analysed for AV 17 by visible spectroscopy at 542 nm (JENWAY 6715, UV/VIS spectrometer, 1.5 nm spectral bandwidth). Each sample was analysed in triplicate with respect to each condition and the standard deviation of these measurements was found to be around ±2%. Based on calibration data, the detection limit was estimated to be around 1 mg L^{-1}.

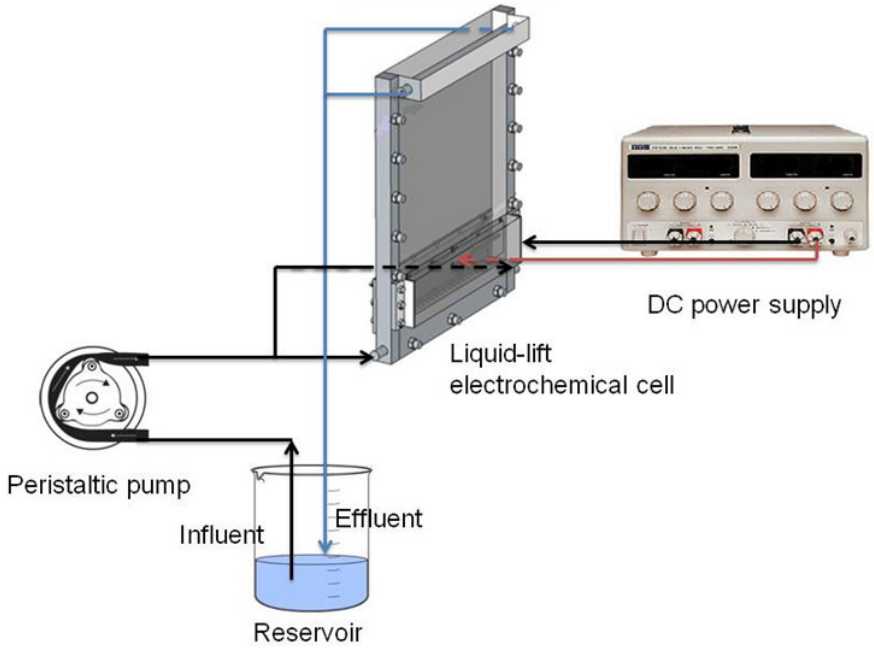

Fig. 2. Schematic diagram of the experimental setup for simultaneous adsorption and electrochemical regeneration of GIC loaded with AV 17 in a liquid-lift electrochemical cell.

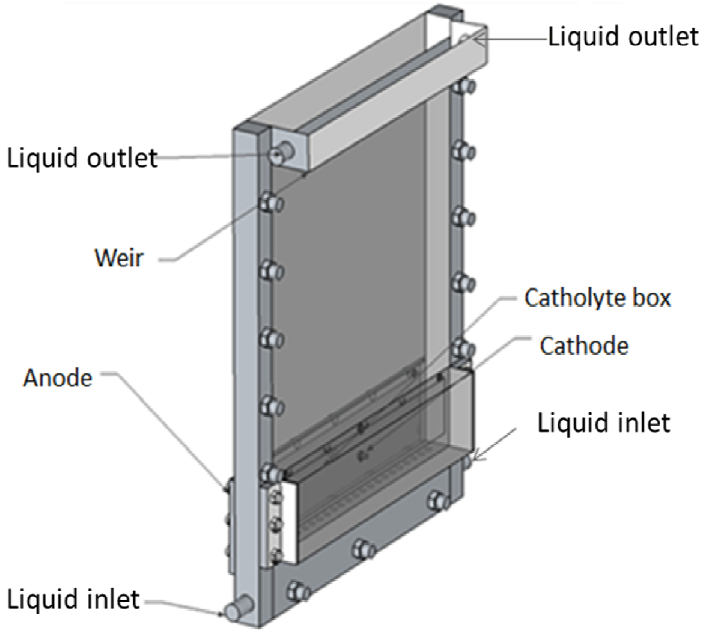

(a)

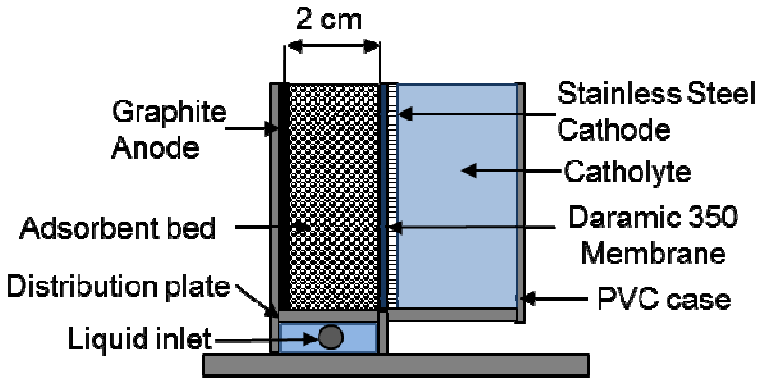

(b)

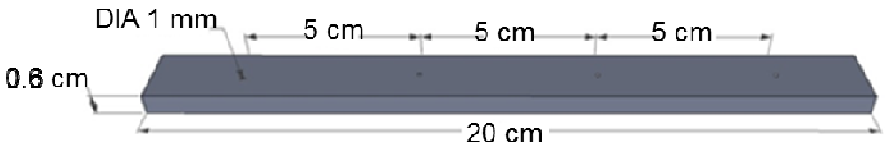

(C)

Fig. 3. Schematic diagram of the batch electrochemical reactor **(a)** isometric view **(a)** cross section of the anode and cathode compartments **(C)** distribution plate

2.3 Flow regime map

Measurement of the minimum spouting velocity, u_{ms}, was accomplished by visually observing the GIC adsorbent bed through the transparent front panel (For these experiments, a second flow visualisation setup was used with the same dimensions as the electrochemical reactor, but without the cathode compartment and with the graphite plate and membrane replaced with a transparent PVC panels in order to observe the flow regime in the anode compartment). The flow regime experiments were carried out for a range of different amounts of GIC, corresponding to different static bed heights in the reactor. The liquid used in this experiment was 105 mg L^{-1} AV 17 solution. The liquid flow rate was increased until spouting conditions were observed. Subsequently, the flow rate was decreased gradually until the spouting fountain collapsed at which point the minimum spouting flow rate was recorded.

Similarly, the minimum fluidizing velocity, u_{mf} , was measured by first increasing the liquid flow rate to until fluidizing bed conditions were observed and then decreasing slowly until the fluidized regime collapsed back to a spouting regime. The liquid flow rate at this transitional point was used to determine the minimum fluidizing velocity.

A flow regime map for the liquid-lift reactor system was constructed by plotting the static bed height versus the superficial liquid velocity of u_{ms} and u_{mf} to identify the stable spouting domain.

3. Results and discussion

3.1 Effect of current density

Fig. 4 shows the effect of current density (based on electrode area) on the concentration of AV 17 for the simultaneous adsorption and electrochemical regeneration experiments. The colour removal was calculated by the following Equation:

$$\text{Colour removal } (\%) = \frac{C_0 - C_t}{C_0} \times 100\% \quad (1)$$

where C_0 is the initial dye concentration and C_t is the remaining dye concentration at given time t. The colour removals obtained were 54.9%, 69.9%, 98.2% and 99.0% for current densities of 1.0, 2.5, 5.0 and 7.5 mA cm^{-2}, respectively after a treatment time of 60 min. The colour removal increased with the current density. However, the colour was almost entirely removed after 60 min for current densities of 5.0 and 7.5 mA cm^{-2}, so further increasing the current density does not increase colour removal significantly.

The advantage of higher current density is that the treatment time for complete colour removal is lower which will reduce the number of cells required resulting in lower capital costs. Fig. 4 shows that there was a linear decrease in AV 17 concentration, corresponding to

a linear increase in colour removal, until the removal approached 98%, (a few mg L^{-1} of AV 17). This observation suggests that the current efficiencies were constant during each experiment (i.e. at each of the applied current densities) for AV 17 concentrations greater than a few mg L^{-1}. However, a linear increase in cell potential with current density was obtained (Fig. 5) and resulted in increased energy consumption (Fig. 6).

The energy consumption per kg AV 17 was calculated by equation (2):

$$\mathrm{EC\ (kwh/kg)} = \frac{\int_0^t I \times U_t dt}{(C_0 - C_t)V} \qquad (2)$$

where I is the applied current (A), $U_t$is cell potential at time t (V), and V is AV 17 solution volume.

The electrical resistance of the cell can be calculated to be 7.92 ohm from the gradient of the trend line in Fig. 5. Thus, there will be a trade-off between capital and operating costs to give an optimum economic solution. Although a current density of 7.5 mA cm^{-2} can remove the colour in slightly less time than a current density of 5 mA cm^{-2} (50 min compared to 60 min), the energy consumption of the former is much higher than the latter (13.2 kwh per kg AV 17 compared to 7.3 kwh per kg AV 17). A current density of 5 mA cm^{-2} for subsequent simultaneous adsorption and electrochemical regeneration experiments. This current density is relatively low but is still consistent with previous work on electrochemical regeneration of GICs, which are typically in the range 5~20 mA cm^{-2}.

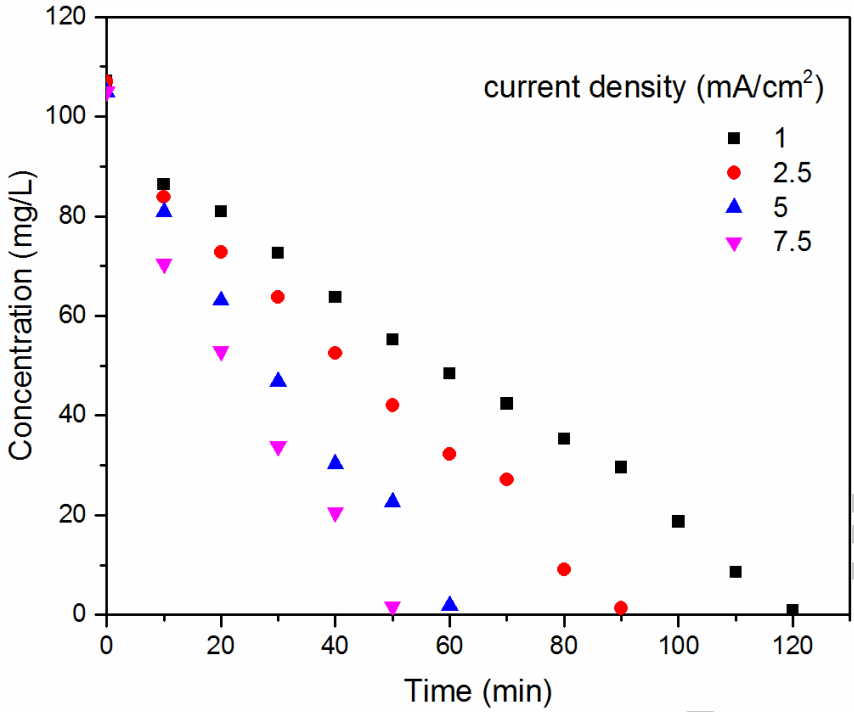

Fig. 4. Treatment time for complete colour removal at different current densities. 4L of AV 17 initial concentration 105 mg L^{-1}; 140g adsorbent; 7.26 ml s^{-1} flow rate; electrode area 100 cm^2.

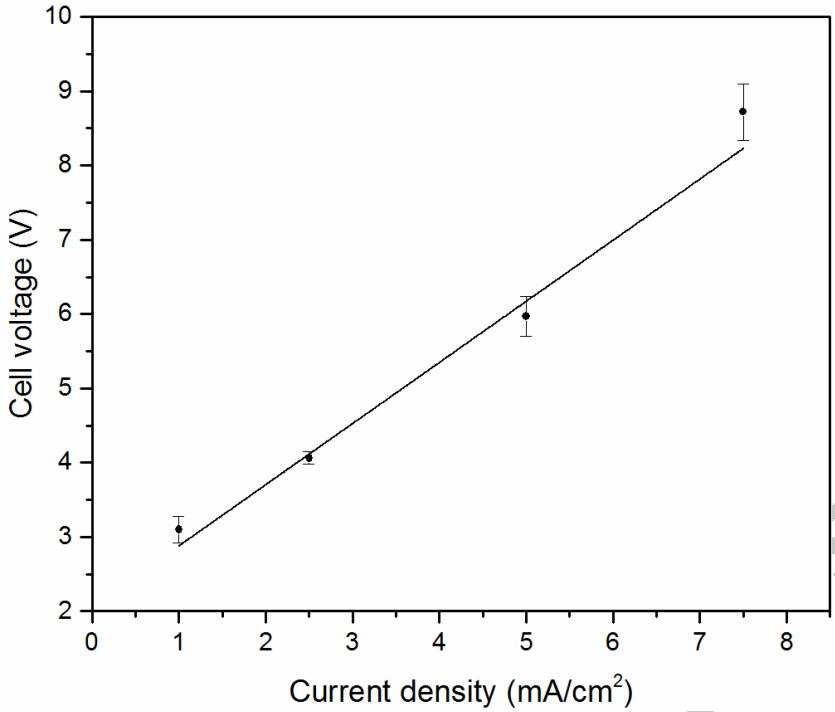

Fig. 5. Cell potential as a function of current density. 4L of AV 17 initial concentration 105 mg L^{-1}; 140g adsorbent; 7.26 ml s^{-1} flow rate; electrode area 100 cm^2.

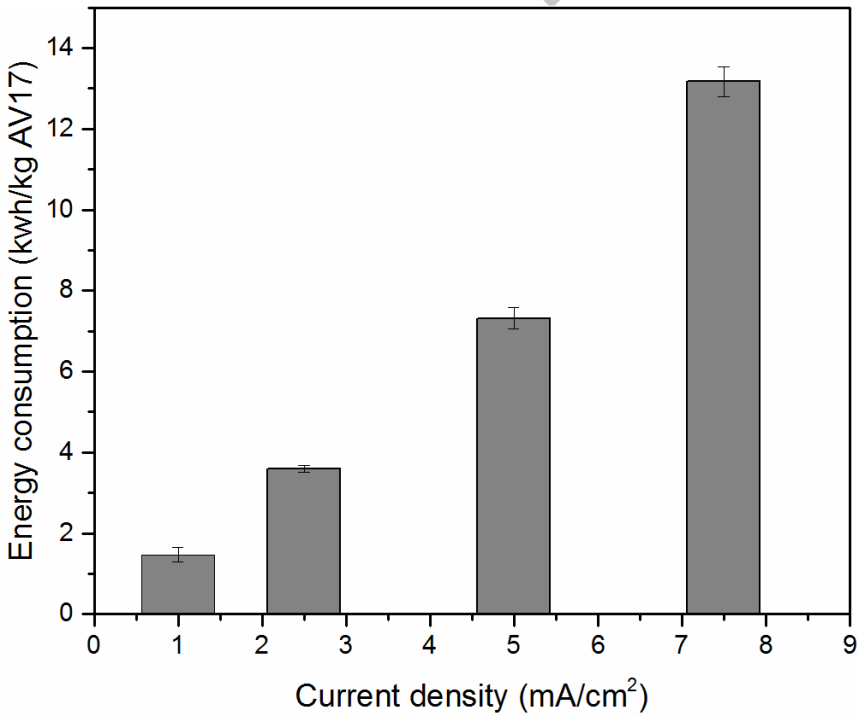

Fig. 6. Energy consumption per kg AV17 removal at different current densities. 4L of AV 17 initial concentration 105 mg L^{-1}; 140g adsorbent; 7.26 ml s^{-1} flow rate; electrode area 100 cm^2.

3.2 Effect of liquid flow rate

To study the effects of AV 17 solution the flow regime on colour removal, a set of experiments was carried out with three flow rates of: 4.61 ml s^{-1} (quiescent bed), 7.26 ml s^{-1} (spouted bed) and 11.6 ml s^{-1} (fluidized bed). A constant current of 0.5A (current density 5mA cm^{-2}) was used in this study. Fig. 7 shows the colour removal obtained as a function of time for each of these flow rates. The colour removal increased with the liquid flow rate. In this work, the colour removals were 64.8%, 98.2%, and 98.9% after 60 min for flow rates of 4.61 ml s^{-1} (static bed), 7.26 ml s^{-1} (spouted bed) and 11.61 ml s^{-1} (fluidized bed), respectively. When the liquid flow rate was increased from 4.61 ml s^{-1} to 7.26 ml s^{-1}, the colour removal rate increased significantly. This can be explained as the increasing the liquid flow rate will decrease the boundary layer and hence the film resistance to mass transfer surrounding the adsorbent particles. However, when the liquid flow rate was increased from 7.26 ml s^{-1} to 11.6 ml s^{-1} (fluidised), the colour removal rate remained almost the same. The film diffusion (external mass transfer) may not be the rate controlling step at this liquid flow rate range. On the other hand, the cell potential increased as the flow rate through the bed was increased (Fig. 8). When flow rate was 4.61 ml s^{-1} and 7.26 ml s^{-1}, the mean cell potential (with some fluctuation) was 5.3 V and 6.1V respectively. The cell potential was much higher (8 to 14V) and was very unstable when the flow rate was increased to 11.6 ml/s (fluidized). This was probably due to the poor inter-particle contact and the intermittent contact of adsorbent particles and the anode current feeder.

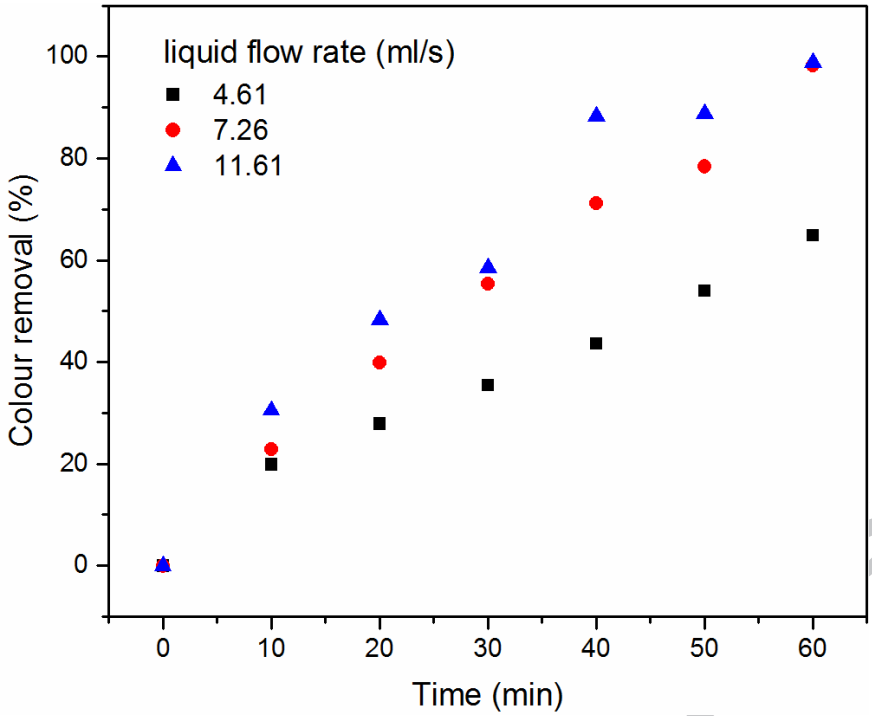

Fig. 7. The AV 17 colour removal at different liquid flow rates. 4L of AV 17 initial concentration 105mg/L; 140g adsorbent; current density 5 mA cm^{-2}; electrode area 100 cm^2.

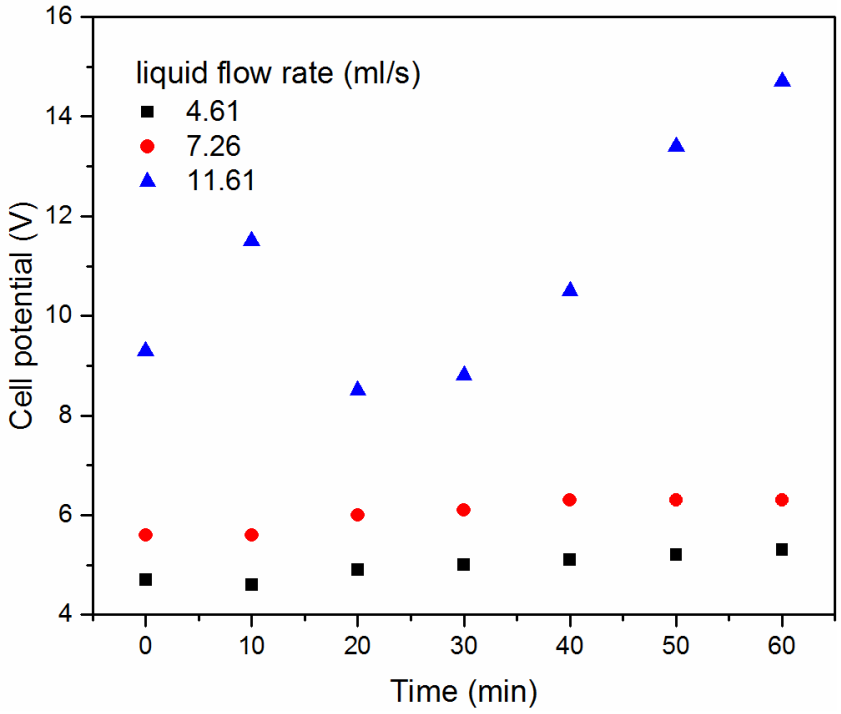

Fig. 8. The cell potential at different liquid flow rates. 4L of AV 17 initial concentration 105mg/L; 140g adsorbent; current density 5 mA cm^{-2}; electrode area 100 cm^2.

3.3 Flow regime map

The flow regime map obtained as on a plot of bed height versus liquid superficial velocity for the water-GIC system is shown in Fig. 9. Three different flow regimes were observed for all bed heights studied: static bed, spouted bed, and fluidized bed. In Fig. 9, the solid lines represent the transition between flow regimes. For bed heights ranging from 3 to 23 cm, all the transitional points were located by varying the liquid flow rate as described in section 2 above. Fig. 9 shows that the minimum spouting velocity , u_{ms}, increases as the bed heights increased. The experimental data were subsequently fitted to equation (3) [27], which is a widely used equation to estimate the minimum spouting velocity.

$$u_{ms} = K\left[\frac{d_{\mathrm{p}}}{D}\right]^{a}\left[\frac{D_i}{D}\right]^{b}\left[\frac{H}{D}\right]^{c}\sqrt{\frac{2gH(\rho_p-\rho_f)}{\rho_f}} \tag{3}$$

where, D_i=diameter of fluid inlet, D=column width, H= bed depth, usually measured as loose–packed static bed depth after spouting, d_p= particle diameter or mean diameter, ρ_p= density of particles, ρ_f= density of fluid, μ= viscosity of fluid, g= gravitational acceleration.

With dimensional analysis, the value of K, a, b and c can be found by applying the method of least squares to experimental data points. The best fits resulted when K, a, b and c were equal to 0.388, 0.869, 0.446, and -0.049 respectively, with a correlation coefficient of 0.986. The 95% confidence intervals for these regression parameters K, a, b and c are (0.383, 0.393), (0.865, 0.872), (0.443, 0.449) and (-0.119, 0.021) respectively.

Fig. 9 shows that the minimum fluidizing velocity, u_{mf}, is approximately independent of bed heights. This phenomenon can be consistent with standard methods of estimating the minimum fluidizing velocity when particle size is very small such as Nyex, which are not correlated to the bed height [28]. Generally, the superficial velocity at minimum fluidizing

conditions, u_{mf}, is given by Equation (4). For very small particles, Equation (4) simplifies to Equation (5).

$$\frac{150(1-\varepsilon_{mf})}{{\varepsilon_{mf}}^3{\Phi_s}^2}\left(\frac{d_p u_{mf}\rho_f}{\mu}\right)+\frac{1.75}{{\varepsilon_{mf}}^3\Phi_s}\left(\frac{d_p u_{mf}\rho_f}{\mu}\right)^2=\frac{{d_p}^3\rho_f(\rho_p-\rho_f)g}{\mu^2} \quad (4)$$

$$u_{mf}=\frac{{d_p}^2(\rho_p-\rho_f)g}{150\mu}\frac{{\varepsilon_{mf}}^3{\Phi_s}^2}{1-\varepsilon_{mf}}, \qquad \mathrm{Re_{p,mf}} < 20 \quad (5)$$

where, ε_{mf} = void fraction in a bed at minimum fluidizing conditions, Φ_s = sphericity of a particle, $\mathrm{Re_{p,mf}}$ = particle Reynolds number at minimum fluidizing conditions.

Unlike the fluidisation velocity, the spouting velocity u_{ms} does vary with the bed height, consistent with previous studies of spouting bed flow regimes [21,22]. For this system there are a broad range of flow rates for which a stable spouting bed can be obtained.

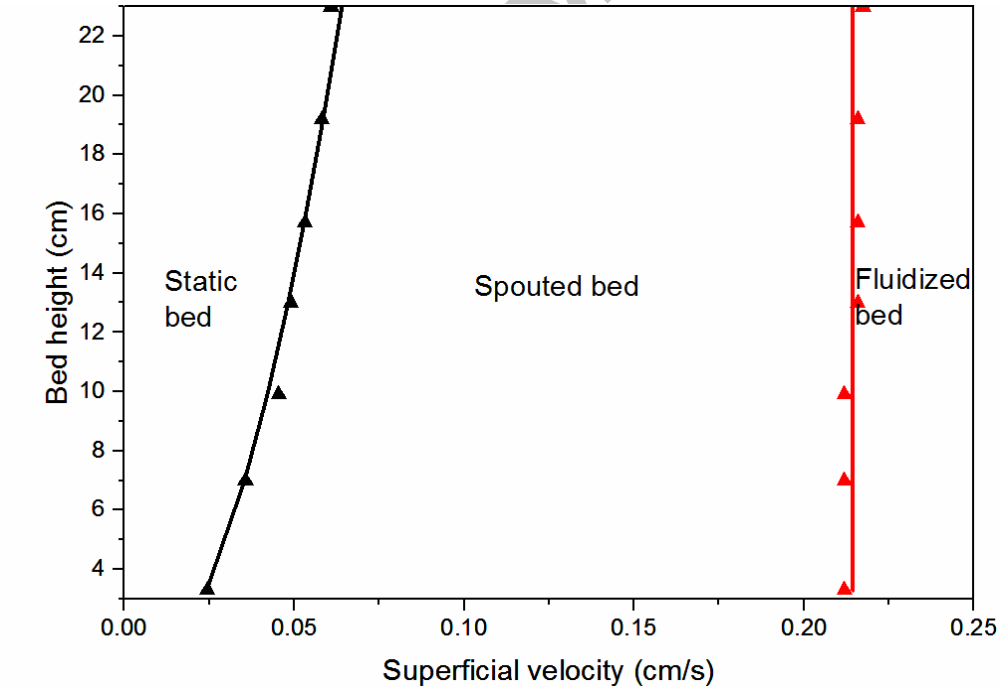

Fig. 9. Flow regime map for adsorbent bed in liquid-lift reactor. The solid lines show the minimum spouting velocity expression (Equation (3)) and minmium fluidizing velocity expression (Equation (4)) fitted to the experimental data (triangles).

3.4 Adsorption and electrochemical regeneration modelling

A model was developed to predict the outlet concentration of pollutant (AV 17), $C_{p,o}$, for a given set of operating conditions. The feed flow of AV 17 aqueous solution enters the adsorption and regeneration reactor from the tank at a constant flow rate Q and at the concentration of AV 17 in the tank, $C_{p,tank}$. The reactor is considered to include an adsorption zone which refers to the volume occupied by liquid spouts region with dispersed particles, and a regeneration zone which refers to the adjacent regions where the adsorbent bed is present as a moving packed bed. The adsorbent circulates between the adsorption and regeneration zones, as shown in Fig. 10.

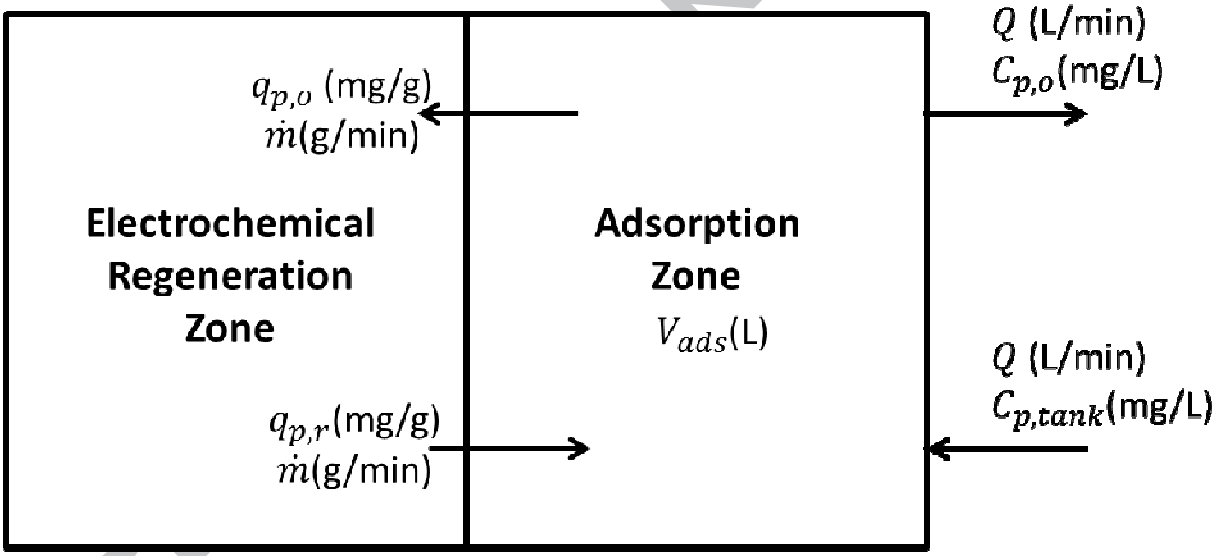

Fig. 10. Schematic representations of the adsorption and electrochemical regeneration processes

The key assumptions used in the model were as follows:

- The tank was assumed to be well mixed with a uniform concentration of AV 17 of C_{tank}.
- Adsorption was assumed to occur in the fluidised spouting regions (adsorption zone) in the anode compartment, and this has a fixed volume V_{ads}.

- The adsorption zone was assumed to be well mixed, with uniform AV 17 concentration in solution $C_{p,o.}$
- All of the adsorbent in the adsorption zone was assumed to have a uniform loading of AV 17 $q_{p,o.}$
- The rate of adsorption was assumed to be controlled by mass transport, with an overall mass transport coefficient $k_L a$. This is also equivalent to first order adsorption kinetics with the mass transfer coefficient replaced by an adsorption rate constant.
- Regeneration was assumed to occur only in the moving packed bed region (regeneration zone) in the anode compartment.
- The adsorbent in the regeneration zone was assumed to have a uniform loading of AV 17 $q_{p,r.}$
- The rate of regeneration was assumed to be Faradic (i.e. proportional to the applied current), but with a current efficiency that was a function of the loading ($q_{p,r}$) in the regeneration zone.
- The rate of exchange of liquid between the adsorption and regeneration zones was assumed to be negligible.
- Adsorbent was assumed to be exchanged with the adsorption zone at a fixed rate $\dot{m}$. This implies that the mass of adsorbent in the regeneration zone was fixed.

A mass balance for the tank gives:

$$\frac{dM_{tank}}{dt} = QC_{p,o} - QC_{p,tank} \tag{6}$$

For adsorption zone, the mass balance for the liquid phase gives:

$$\frac{dM_{ads,l}}{dt} = QC_{p,tank} - QC_{p,o} - V_{ads}k_L a\left(C_{p,o} - C_p^*\right) \tag{7}$$

and for the adsorbent phase:

$$\frac{dM_{ads,s}}{dt} = \dot{m}q_{p,r} - \dot{m}q_{p,o} + V_{ads}k_L a\left(C_{p,o} - C_p^*\right) \tag{8}$$

where M_{tank}, $M_{ads.l}$ and $M_{ads,s}$ are the mass of AV 17 in the tank, adsorption zone liquid phase and adsorption zone solid phase respectively. $\dot{m}$ is the mass flow rate (g min^{-1}) of adsorbent circulating between the adsorption zone and the electrochemical regeneration zone,

and $q_{p,o}$ and $q_{p,r}$ are the loading of AV 17 on the adsorbent (mg g^{-1}) leaving and returning to the adsorption zone respectively. V_{ads} is the volume of adsorption zone. $k_L a$ is the mass transfer coefficient from the liquid to the adsorbent interface, C_p^* is the liquid phase concentration at the liquid-adsorbent interface (mg L^{-1}).

Assuming the adsorption follows a Langmuir isotherm:

$$q_{p,o} = \frac{bK_L C_p^*}{1 + bC_p^*} \tag{9}$$

Then

$$C_p^* = \frac{q_{p,o}}{bK_L - bq_{p,o}} \tag{10}$$

where b and K_L are Langmuir constants obtained from adsorption isotherm experiment [16,29].

From Faraday's law, for electrochemical regeneration zone gives:

$$\frac{dM_{reg}}{dt} = \dot{m}q_{p,o} - \dot{m}q_{p,r} - I\frac{\mathrm{M_w}}{nF}\eta \tag{11}$$

$$\eta = \eta_{max}\left(\frac{q_{p,r}}{q_{p,half} + q_{p,r}}\right) \tag{12}$$

where M_{reg} is the mass of AV17 in the electrochemical regeneration zone, I is the applied current (A), M_w is molecular weight of AV 17, n is number of electrons required per molecule of AV 17 oxidized, F is Fraday's constant, 96487 C mol^{-1} and η is current efficiency, which is assumed to be a simple function of the amount of adsorbate (AV 17) on the adsorbent (GIC) from Equation (12). $q_{p,half}$ is an assumed constant which gives a constant current efficiency at relatively high loadings whilst the efficiency asymptotes to zero at zero loading.

This coupled set of mass balance equations (6), (7), (8) and (11) represent an initial value problem which can be integrated from the conditions at $t = 0$ to yield the variation in the

adsorbate concentration with time recursively. Thus for given flow rate Q, feed concentration $C_{p,tank}$, V_{ads}, b, and K_L the outlet concentration $C_{p,o}$ can be determined from a numerical solution of Equations (6)~(12). A simple Euler's method was used for the integration, and a time interval of 30 s was found to be sufficiently small to obtain accurate results. The feed concentration in the tank was found to change by less than 0.1% during the first 40 minutes when the time step was halved, confirming that a more accurate integration scheme was not required. The model includes four parameters, $k_L a$, $\dot{m}$, η_{max} and $q_{p,half}$, and these parameters were obtained by fitting the data to the experimental data using a non-linear least squared error method. All the ordinary differential equations (Equation (6), (7), (8) and (11)) can be calculated from time t=0 to t=60 min with 30 s time intervals. Fig. 11 shows a comparison of outlet concentration, $C_{p,o}$, obtained from the experimental data and the fitted model. The value of the fitted parameters are shown in Table 2. Each parameter was examined using "sensitivity analysis" to determine relative importance of the factor in influencing the model from Equation (13). The "sensitivity analysis" of each parameter in Table 2. was conducted by making a small change Δx_i in parameter x_i, and determining the change in the sum of the squared error, $\Delta f(x_i) = f(x_i + \Delta x_i) - f(x_i)$, where $f(x_i)$ the sum of the square of the error between the experimental $C_{p,o}$ values and the model calculated values using parameter values x_i. The corresponding sensitivity coefficient was obtained using Equation (14). The "sensitivity analysis" indicated that compared to $\dot{m}$ (the mass flow rate of adsorbent circulating between the adsorption zone and the electrochemical regeneration zone) the parameter $k_L a$, η_{max} and $q_{p,half}$ had only small effects on the model. The results shown in Fig. 11 indicate that the model gives a good prediction of the outlet concentration for the range of conditions studied.

$$f(x_i) = \sum_{i=1}^{n} \left[C_{p,o,observed}(x_i) - C_{p,o,calculated}(x_i) \right]^2 \quad (13)$$

The sensitivity coefficient is calculated using:

$$\Phi_i = \frac{\%\Delta f(x_i)}{\%\Delta x_i} \quad (14)$$

Table 2

Values of the parameters used in Equation (6)~(12)

Parameter	Value	Unit	Sensitivity coefficient
$k_L a$	2.85	min^{-1}	0.21
$\dot{m}$	20.0	g min^{-1}	53.7
η_{max}	0.75	–	0.015
$q_{p,half}$	0.0079	mg g^{-1}	0.43

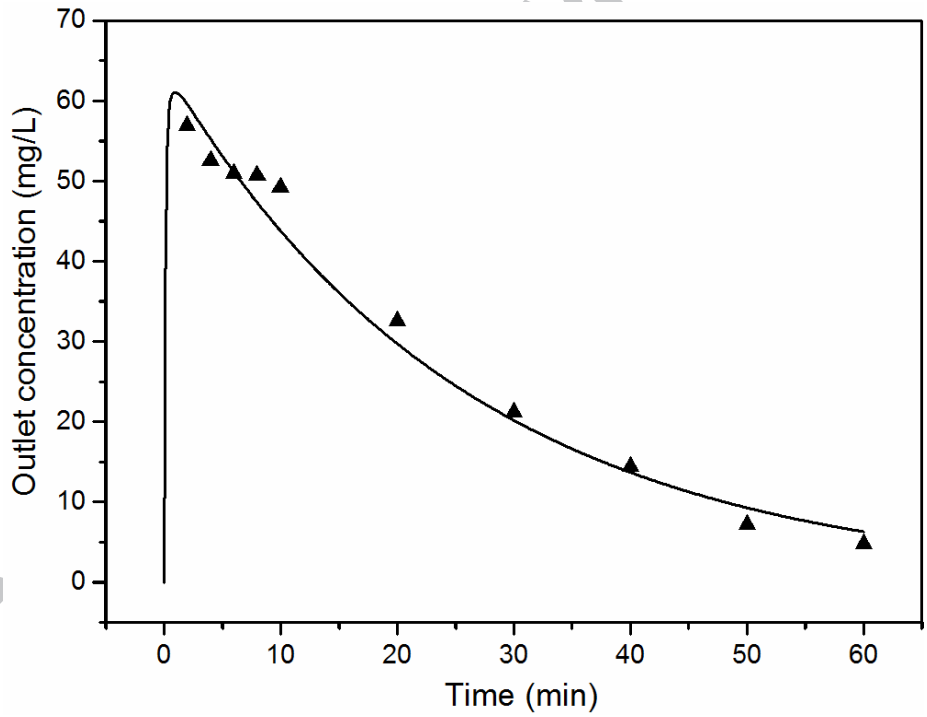

Fig. 11. Modelling of the outlet concentration of the adsorption and electrochemical regeneration reactor. The solid line show the modelling predictions fitted to the experimental data (triangles).

Conclusions

Electrochemical regeneration of GIC loaded with AV 17 was investigated in a novel spouted bed reactor. The effect of the operating conditions, including the current density and the liquid flow rate, on the system performance of the process was investigated. As expected, higher current density increased the rate of treatment, but increased the energy consumption. It was shown that a current density of 5 mA cm^{-2} is a good compromise between the rate of colour removal and energy consumption. It was found that good performance for simultaneous adsorption and electrochemical regeneration can be achieved by forming a spouted bed in the electrochemical reactor, e.g. with a liquid flow rate of 7.26 ml s^{-1}. Under those conditions, around 98% of AV17 was removed from 4 L of 100 ppm AV 17 solution within 60 min by simultaneous adsorption and electrochemical regeneration, using an electrode area of 100 cm^2 and 140 g of GIC adsorbent. The energy consumption was 7.32 kWh per kg of AV 17.

The spouted bed region defined an interesting operating domain of liquid flow rate for simultaneous adsorption and regeneration. Under spouting bed conditions, there are fluidized spouts where the liquid and adsorbent are turbulent and adsorption can occur, along with zones with of moving packed bed providing a continuous conductive pathway for the regeneration current. The conditions to have a stable spouted bed, between the minimum spouting velocity and the minimum fluidizing velocity, were determined and plotted on a flow regime map.

For batch simultaneous adsorption and electrochemical regeneration system, a four-parameter model was proposed and fitted to the experimental data. A sensitivity analysis indicated that the circulation rate of the adsorbent, $\dot{m}$, was the key parameters effecting

treatment performance. Experimental data and the fitted model predictions of the dye removal achieved were found to be in good agreement.

The technical feasibility of the adsorption and electrochemical regeneration using a two-phase liquid spouted bed reactor has been demonstrated by the results presented in this paper. The potential benefit of using such a reactor is likely to be lower energy consumption, simpler reactor configurations compared to conventional three-phase gas-liquid-solid reactor. However significant further work is required before its commercial acceptance.

Acknowledgements

The authors acknowledge the financial and material support received from the Arvia Technology Ltd. and the University of Manchester. Special thanks to Mr. Andrew Evans from School of Chemical Engineering and Analytical Science Workshop for the fabrication of the experimental reactor.

References

[1] R. Berenguer, J. P. Marco-Lozar, C. Quijada, D. Cazorla-Amoros, E. Morallon, Comparison among chemical, thermal, and electrochemical regeneration of phenol-saturated activated carbon, Energy & Fuels. 24 (2010) 3366-3372.

[2] R.Sivaraj, C. Namasivayam, K. Kadirvelu, Orange peel as an adsorbent in the removal of Acid violet 17 (acid dye) from aqueous solutions, Waste Management. 21 (2001) 105-110.

[3] R.S. Juang, F.C. Wu, R.L. Tseng, Mechanism of adsorption of dyes and phenols from water using activated carbons prepared from plum kernels, Journal of Colloid and Interface Science. 227 (2000) 437-444.

[4] N. Thinakaran, P. Baskaralingam, M. Pulikesi, P. Panneerselvamc, S. Sivanesan, Removal of Acid Violet 17 from aqueous solutions by adsorption onto activated carbon prepared from sunflower seed hull, Journal of Hazardous Materials. 151 (2008) 316-322.

[5] N.W. Brown, E.P.L. Roberts, A.A. Garforth, R.A.W. Dryfe, Electrochemical regeneration of a carbon-based adsorbent loaded with crystal violet dye, Electrochimica Acta. 49 (2004) 3269-3281.

[6] E. Sabio, E. Gonzalez, J.F. Gonzalez, C.M. Gonzalez-Garcıa, A. Ramiro, J. Ganan, Thermal regeneration of activated carbon saturated with p-nitrophenol, Carbon. 42 (2004) 2285-2293.

[7] X. Quan, X.Liu, L.Bo, S. Chen, Y. Zhao, X. Cui, Regeneration of acid orange 7-exhausted granular activated carbons with microwave irradiation, Water Research. 38 (2004) 4484-4490.

[8] J.L. Lim, M. Okada, Regeneration of granular activated carbon using ultrasound, Ultrasonics Sonochemistry. 12 (2005) 277-282.

[9] G.M.Walker, L.R. Weatherley, Bacterial regeneration in biological activated carbon systems, Process Safety and Environmental Protection. 76 (1998) 177-182.

[10] Toledo, L.C., et al., Application of Fenton's reagent to regenerate activated carbon saturated with organochloro compounds. Chemosphere. 50 (2003) 1049-1054.

[11] R.V.Shende, V.V. Mahajani, Wet oxidative regeneration of activated carbon loaded with reactive dye, Waste Management. 22 (2002) 73-83.

[12] H. Zhang, Regeneration of exhausted activated carbon by electrochemical method, Chemical Engineering Journal. 85 (2002) 81-85.

[13] R.M. Narbaitz, A. Karimi-Jashni, Electrochemical regeneration of granular activated carbons loaded with phenol and natural organic matter, Environmental Technology. 30 (2009) 27-36.

[14] L. Wang, N. Balasubramanian, Electrochemical regeneration of granular activated carbon saturated with organic compounds. Chemical Engineering Journal. 153 (2009) 763-768.

[15] C.H. Weng, M.C. Hsu, Regeneration of granular activated carbon by an electrochemical process, Separation and Purification Technology. 64 (2008) 227-236.

[16] F.M. Mohammed, E.P.L. Roberts, A. Hill, A.K. Campen, N.W. Brown, Continuous water treatment by adsorption and electrochemical regeneration, Water Research. 45 (2011) 3065-3074.

[17] G. Chen, Electrochemical technologies in wastewater treatment, Separation and Purification Technology. 38 (2004) 11-41.

[18] V.S. Sutkar, N.G. Deen, J.A.M. Kuipers, Spout fluidized beds: Recent advances in experimental and numerical studies, Chemical Engineering Science. 86 (2013) 124-136.

[19] K.B.Mathur, P.E.Gishler, A technique for contacting gases with coarse solid partcles, AIChE Journal. 1(2) (1955) 157-164.

[20] H. Nagashima, K. Suzukawa, T. Ishikura, Hydrodynamic performance of spouted beds with different types of draft tubes, Particuology. 11(5) (2013) 475-482.

[21] M.L. Passos, A.S. Mujumdar, V.S.G. Raghavan, Prediction of the maximum spoutable bed height in two-dimensional spouted beds, Powder Technology. 74 (1993) 97-105.

[22] N.Epstein, J.R.Grace, Spouted and Spout-Fluid Beds, 1st ed., Cambridge University Press. (2011).

[23] M.H. El-Naas, S. Al-Zuhair, S. Makhlouf, Continuous biodegradation of phenol in a spouted bed bioreactor (SBBR). Chemical Engineering Journal. 160 (2010) 565-570.

[24] S.N. Hussain, E.P.L. Roberts, H.M.A. Asghar, A.K. Campen, & N.W. Brown, Oxidation of phenol and the adsorption of breakdown products using a graphite adsorbent with electrochemical regeneration, Electrochimica acta. 92 (2013), 20-30.

[25] K. Nkrumah-Amoako, E.P.L. Roberts, N.W. Brown, & S.M. Holmes, The effects of anodic treatment on the surface chemistry of a Graphite Intercalation Compound, Electrochimica Acta, 135 (2014), 568-577.

[26] M. Streat, J.W. Patrick, M.J.C. Perez, Sorption of phenol and para-chlorophenol from water using conventional and novel activated carbons. Water Research. 29 (1995) 467-472.

[27] S.W.M. Wu, C. Jim Lim, N. Epstein, Hydrodynamics of spouted beds at elevated temperatures, Chemical Engineering Communications, 62 (1987) 251-268.

[28] D. Kunii, O. Levenspiel, Fluidization Engineering, Second Ed., Butterworth-Heinemann, Boston. (1991) 61-94.

[29] D.Liu, Water treatment by adsorption and electrochemical regeneration–development of a liquid-lift reactor,University of Manchester, PhD thesis. (2015) 94-101.

Highlights

- A two-phase reactor is a promising alternative to traditional three-phase reactor.
- The spouted bed region defined an interesting operating domain.
- Study of current density and the liquid flow rate on the system performance.
- A model is developed for the adsorption and electrochemical regeneration process.